


Anuran heart development and critical developmental periods: A comparative analysis of three neotropical anuran species

María Teresa Sandoval¹  | Romina Gaona¹ | Lucila Marilén Curi^{2,3} |
Fernanda Abreliano¹ | Rafael Carlos Lajmanovich^{2,4} | Paola Mariela Peltzer^{2,4}

¹Facultad de Ciencias Exactas y Naturales y Agrimensura, Embriología Animal, Universidad Nacional del Nordeste, Corrientes, Argentina

²Consejo Nacional de Investigaciones Científicas Técnicas (CONICET), Buenos Aires, Argentina

³Instituto de Ictiología del Nordeste (INICNE), Facultad de Ciencias Veterinarias, Universidad Nacional del Nordeste (FCV, UNNE), Corrientes, Argentina

⁴Laboratorio de Ecotoxicología, Facultad de Bioquímica y Ciencias Biológicas, Universidad Nacional del Litoral (FBCB-UNL), Santa Fe, Argentina

Correspondence

María Teresa Sandoval Facultad de Ciencias Exactas y Naturales y Agrimensura, Embriología Animal, Universidad Nacional del Nordeste, Av. Libertad 5470 (3400), Corrientes, Argentina.

Email: tetesandoval@hotmail.com

Funding information

CAI+D, Grant/Award Number: 50620190100036LI; SGCyT-UNNE, Grant/Award Number: 20F002

Abstract

The heart begins to form early during vertebrate development and is the first functional organ of the embryo. This study aimed to describe and compare the heart development in three Neotropical anuran species, *Physalaemus albonotatus*, *Elachistocleis bicolor*, and *Scinax nasicus*. Different Gosner Stages (GS) of embryos (GS 18–20) and premetamorphic (GS 21–25), prometamorphic (GS 26–41), and metamorphic (GS 42–46) tadpoles were analyzed using stereoscopic microscopy and Scanning Electronic Microscopy. Heart development was similar in the three analyzed species; however, some heterochronic events were identified between *P. albonotatus* and *S. nasicus* compared to *E. bicolor*. In addition, different patterns of melanophores arrangement were observed. During the embryonic and metamorphic periods, the main morphogenetic events occur: formation of the heart tube, regionalization of the heart compartments, development of spiral valve, onset of heartbeat, looping, and final displacement of the atrium and its complete septation. Both periods are critical for the normal morphogenesis and the correct functioning of the anuran heart. These results are useful to characterize the normal anuran heart morphology and to identify possible abnormalities caused by exposure to environmental contaminants.

KEYWORDS

anuran, cardiogenesis, interspecific variations

1 | INTRODUCTION

Heart development is a highly conserved process in all vertebrate organisms (Warkman & Krieg, 2007). The heart has been traditionally defined as the chambered pumping organ of vertebrates (Xavier-Neto et al., 2010) and is the first functional organ of vertebrate embryos (Warkman & Krieg, 2007). The cell precursors of the primary vertebrate heart tube originate during early-mid

gastrulation. In the chick, from their original midline primitive streak location, these cells move antero-laterally as a dense mass of mesodermal mesenchyme to form the primary heart fields. These bilateral primary heart fields differentiate into the endocardial and myocardial lineages, move to the midline and converge medially to give rise to a single linear heart tube (Colas et al., 2000), which contains the outlines of the ventricle and atrioventricular and atrial regions. To complete the

embryonic heart structure, myocardial precursors are added to the anterior (arterial) and posterior (venous) heart poles and give rise to the inflow and outflow compartments, respectively (Pérez-Pomares et al., 2009). The linear heart tube is a transient structure that adopts a rightward spiral form in a process called cardiac looping. During looping, the future ventricles become balloon outwards, and the atrial region and sinus venosus move dorsally and cranially. This process brings the primitive compartments into the alignment necessary for their future integration (Harvey, 2002). It is, therefore, regarded as the key process of heart morphogenesis, with several forms of congenital cardiac malformations probably resulting from disturbances in cardiac looping (Männer, 2009).

The chronological sequence of heart development has been well documented in birds and mammals (Bartman & Hove, 2005; Opitz & Clark, 2000; Wittig & Münsterberg, 2016, 2020). The heart primordium forms at 29 hr of incubation in chicken, and at about 3 weeks of gestation in humans. The heartbeat initiates early in the development because of an intrinsic contractile capacity conferred by the presence of sodium–calcium pumps on the muscle cell membrane of the heart primordium (Linask et al., 2001; Tyser & Srinivas, 2020). Four compartments are distinguished in the heart linearly located along the anterior–posterior axis: an outflow tract, a ventricle, an atrium, and a sinus venosus. They are visible from 33 to 36 hr in chick embryos, and from 5 weeks in human embryos. Subsequently, cardiac looping leads to important topographic changes. The ventricle moves in a ventral-caudal and right direction, whereas the sinus venosus and the atrium move in a dorsal, cranial, and left direction. These events transform the original anterior–posterior polarity of the heart primordium into the typical right–left polarity of the vertebrate heart (Miquerol & Kelly, 2013).

The heart development of anurans was described for a few species, with *Xenopus laevis* being the most widely studied (Hempel & Kühn, 2016; Mohun et al., 2000; Sater & Jacobson, 1989; Warkman & Krieg, 2007). In this species, the heart originates from two bilateral patches of mesoderm located on the dorsal side of the embryo at the onset of gastrulation. Gastrulation movements cause the heart patches to move dorso-anteriorly; then, during neurulation, they migrate to the ventral midline of the pharynx, where they fuse. The fusion results in a simple linear tube, which undergoes the looping and remodeling processes of the heart morphogenesis (Warkman & Krieg, 2007). Heart development was also analyzed in *Rana temporaria* (Viertel & Richter, 1999), *Rhinella arenarum* (Paz, 1987), and *Physalaemus biligonigerus* (Casco & Lajmanovich, 1999). These reports showed a

conserved morphogenetic pattern of anuran heart development during the embryonic and premetamorphic periods; however, there is scarce information regarding the prometamorphic and metamorphic development stages.

Heart development of model organisms, such as amphibians, may be useful to explain the etiology of congenital malformations in humans (Brand, 2003; Nemer, 2008). Several studies support the similarity in genetic expression among vertebrates during heart development (Hempel & Kühn, 2016; Olson & Srivastava, 1996; Yunqing et al., 2000). Sissman (1970) identified 49 events of heart development in different species of vertebrates and highlighted the importance of ontogenetic changes in the size of cardiac structures and temporal maturation sequences. This author also referred to critical periods or “windows” of development, that is, the periods when exposure to a teratogenic agent could induce a specific malformation (Ozeki et al., 1999). Heart abnormalities were reported for fishes (Incardona & Scholz, 2017; Praskova et al., 2014; Watson et al., 2014) and anuran species (Cuzziol Boccioni et al., 2020; Lenkowski et al., 2008; Peltzer et al., 2019, 2022) exposed to agrochemicals, such as atrazine, chlorpyrifos, dichlorvos, and diazinon, and emerging contaminants such as dexamethasone, diclofenac, and chlorine dioxide. Similar findings were reported for humans chronically exposed to several agrochemicals (Sekhatha et al., 2016). Jones-Costa et al. (2018) demonstrated the relevance of employing morphological, physiological, and cellular features of the heart as biomarkers to evaluate the effects of xenobiotics in anuran tadpoles.

Amphibians exhibit an extremely high diversity in morphology, physiology, and life history, as well as in heart morphology (Olejnickova et al., 2021). The present study aimed to describe and compare the heart development during the embryonic period and premetamorphic, prometamorphic, and metamorphic larval periods of three Neotropical anuran species: *P. albonotatus*, *Elachistocleis bicolor*, and *Scinax nasicus*, and to identify the critical periods of heart development.

2 | MATERIALS AND METHODS

2.1 | Selected species

P. albonotatus (Anura: Leptodactylidae), *E. bicolor* (Anura: Microhylidae), and *S. nasicus* (Anura: Hylidae) are common species in the Neotropical region, including mid-western, southern, and southeastern Brazil, southern Uruguay, Paraguay, northeastern Argentina, and eastern Bolivia. In Argentina, they coexist in Chaco, Formosa,

Misiones, Corrientes, Entre Ríos, Santa Fe, and Buenos Aires provinces (Zaracho et al., 2011) and they are categorized as “not threatened” (Vaira et al., 2012). The species were selected mainly because they belong to different families and phylogenetic lineages (Pyron & Wiens, 2011) and have different tadpoles types (Orton, 1953). *P. albonotatus* and *S. nasicus* have type IV tadpoles, whereas *E. bicolor* has type II tadpoles. In addition, the embryos and tadpoles of these species are good models because they are easily maintained under laboratory conditions.

2.2 | Embryos and tadpoles

Clutches with embryos of *P. albonotatus* and *E. bicolor*, and prometamorphic tadpoles of *S. nasicus* were collected from temporary and semi-permanent ponds of a suburban area near the Campus of Universidad Nacional del Nordeste (UNNE) (27° 27' 58" S 58° 47' 04" W) and the locality of Perichón (27° 24' 58" S 58° 45' 03" W) in Corrientes province, Argentina. It was not possible to analyze embryonic and prometamorphic stages of *S. nasicus* due to the difficulty to find eggs of this species. Samplings were conducted from August to December, during two annual periods (2017 and 2018). Clutches were obtained by hand and tadpoles were trapped using a capture net. The samples were transported to the laboratory in plastic flasks containing water from the collection sites mixed with dechlorinated tap water. After acclimatization, embryos and tadpoles were raised in plastic containers with dechlorinated tap water and fed with boiled lettuce ad libitum.

A total of 180, 125, and 160 embryos and tadpoles at different stages of development of *P. albonotatus*, *E. bicolor*, and *S. nasicus*, respectively, were analyzed. For each species, a set of 10 specimens per stage were euthanized by an overdose of 5% ethyl aminobenzoate solution (Muelitas[®]) added to the rearing water, according to the American Veterinary Medical Association (Leary et al., 2013). After that, embryos and tadpoles were fixed in a 10% formalin solution. This protocol was approved by the Ethics Committee of the Facultad de Ciencias Exactas y Naturales y Agrimensura - UNNE (Res. 0756/18 CD). The developmental stages of embryos and tadpoles were identified according to Gosner's table (Gosner, 1960) and were referred to as GS.

2.3 | Macroscopic heart examination

Embryos and tadpoles were dissected to characterize heart morphology. Moreover, a cross-section of the

atrium heart of metamorphic larvae (GS 42–46) was performed to analyze the atrial septation. The observations were made under a Leica ES2 stereoscopic microscope and photographs were taken with a mounted digital camera. Images were edited with the Leica Application Suite (LAS) EZ software and the ImageJ 1.48v software (Schneider et al., 2012).

Premetamorphic and early prometamorphic tadpoles of *P. albonotatus* were analyzed with a Scanning Electron Microscope (SEM) due to their small size. The samples were prepared following the conventional method for SEM. They were washed with a 0.1 M phosphate buffer solution, dehydrated in increasing solutions of acetone and distilled water (12.5; 25; 50; 75; 100%), dried by critical point method in liquid carbon dioxide and coated with gold–palladium complex (Sorrivas de Lozano & Morales, 1986). The observations were made using a SEM JEOL JSM-5800 LV belonging to the Secretaría General de Ciencia y Técnica Universidad del Nordeste (SGCyT-UNNE).

Four anuran development periods were analyzed based on the classification provided by Lavilla and Rougés (1992): embryonic period (GS 18–20), premetamorphic larval period (GS 21–25), prometamorphic larval period (GS 26–41), and metamorphic larval period (GS 42–46). Heart morphology and development, and aortic arches configuration were described according to Viertel and Richter (1999), Mohun et al. (2000), McIndoe and Smith (1984), and Kolker et al. (2000).

A morphogenetic pattern of heart development was described for each species and patterns were compared among species.

The critical periods of heart development were determined as the periods when the main morphogenetic events of heart development occur, based on the criteria proposed by Ozeki et al. (1999).

3 | RESULTS

3.1 | Heart morphology

The main morphogenetic events of heart development during the embryonic period and the premetamorphic, prometamorphic, and metamorphic larval periods in the three analyzed species are summarized and compared in Table 1.

3.1.1 | *Physalaemus albonotatus*

Embryonic period

At GS 18, a linear heart tube was recognized. At GS 19, the onset rightward looping of the heart tube was

TABLE 1 Comparative summary of heart development events of *Physalaemus albonotatus*, *Elachistocleis bicolor*, and *Scinax nasicus* during embryonic and larval periods

	GS	<i>P. albonotatus</i>	<i>E. bicolor</i>	<i>S. nasicus</i>
Embryonic period	18	Formation of the heart tube.	N/D	N/D
	19	Early looping. Inflow tract, ventricle and outflow tract distinguishable. Onset of heartbeat.	Early looping. Inflow tract, ventricle and outflow tract distinguishable.	N/D
	20	Advanced looping.		N/D
	21–24	Sinus venosus and atrium in dorsal and posterior position respect to the ventricle. Parietal pericardium distinguishable.		N/D
Premetamorphic and prometamorphic larval periods	25	Carotid arch, systemic arch, and pulmocutaneous arch distinguishable. Endocardial trabeculae visible in the ventricle. Spiral valve visible in the outflow tract.		N/D
	30–31	Growth of the atrium.		Prominent ventricle.
	38	Atrium in dorso-posterior position respect to the ventricle.	Atrium in dorso-anterior position respect to the ventricle.	Sinus venosus and atrium in dorso-posterior position respect to the ventricle.
	41	Rounded ventricle.	Irregular, oblong or rounded ventricle.	Irregular ventricle.
	42	Single atrium.		
Metamorphic larval period	43	Single atrium.	Complete atrium septation.	
	44–46	Melanophores on the surface of aortic arches, outflow tract, atrium, and sinus venosus. No melanophores on the surface of the ventricle. Abundant melanophores in the parietal pericardium.	No melanophores on the surface of aortic arches, outflow tract, atrium, and sinus venosus. Scarce melanophores on the surface of the ventricle. No melanophores in the parietal pericardium	Abundant dendritic melanophores on the surface of aortic arches, outflow tract and ventricle. No melanophores on the surface of sinus venosus and atrium. Abundant melanophores in the parietal pericardium.
		Atrium in dorso-anterior position respect to the ventricle. Complete atrium septation. Left and right atriums distinguishable. Sinus venosus in dorsal position respect to atriums.		
		Regression of internal gill, anatomic and topographic changes of aortic arches.		

Abbreviations: GS, Gosner stages; N/D, No data available.

observed and the outflow tract, the ventricle, and the inflow tract were recognized (Figure 1a). The heartbeat was observed in vivo.

Premetamorphic larval period

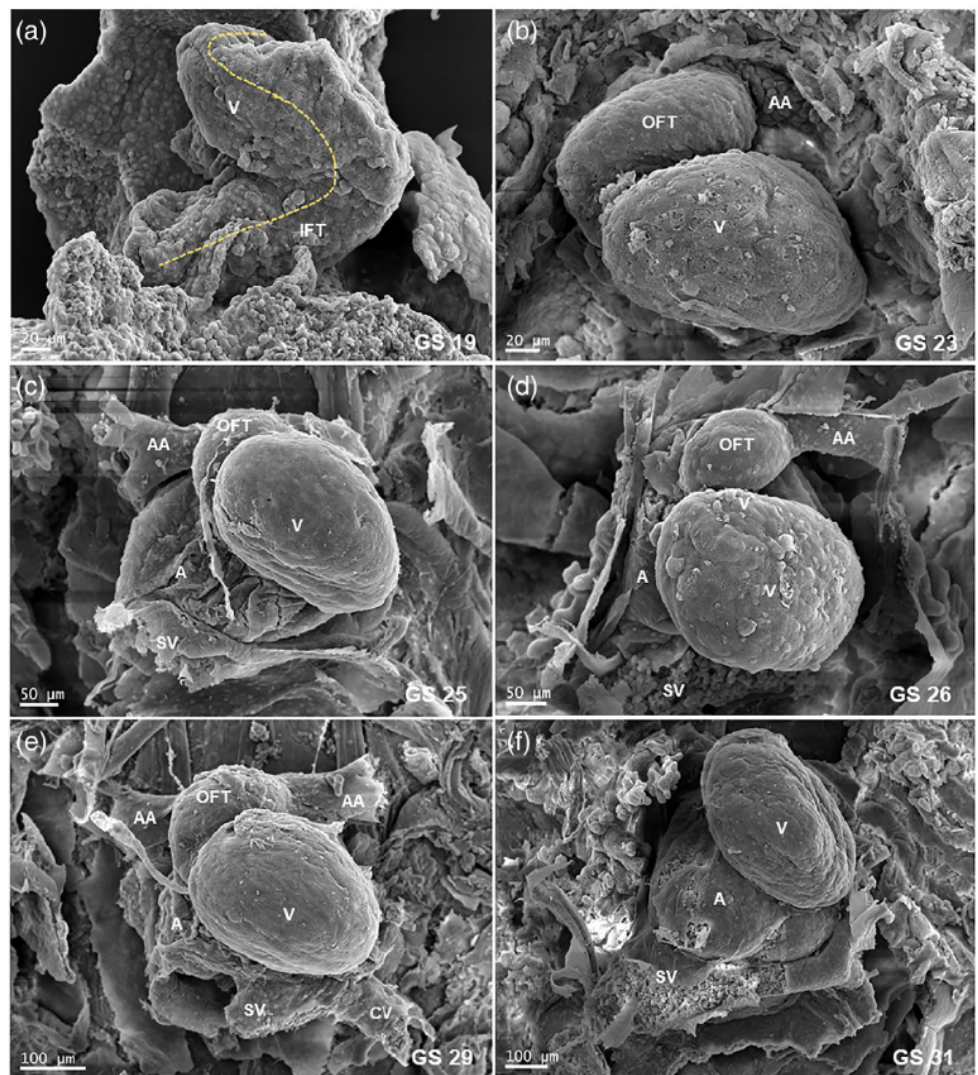
The ventricle and the outflow tract appeared as conspicuous and well-developed compartments from GS 21 to 23 (Figure 1b). The atrium and the sinus venosus were located dorsally to the ventricle and were not visible in ventral view. From GS 24, the parietal pericardium was observable as a thin translucent membrane covering the

entire heart. At GS 25, the sinus venosus and atrium were observed as well-developed and conspicuous compartments in dorso-posterior position with respect to the ventricle (Figure 1c). Under stereoscopic microscope, cardiac trabeculae were visible in the ventricle and a few scattered dendritic melanophores were observed in the parietal pericardium.

Prometamorphic larval period

The topography of the heart compartments between GS 26 and 37 remained similar to that observed at GS

FIGURE 1 Scanning electron microscope microphotographs of the heart morphology of *Physalaemus albonotatus* during embryonic (a), premetamorphic (b, c), and prometamorphic (d–f) larval periods. (a) Note the rightward looping of the heart tube (pointed out with yellow dotted lines). (c–f) Note the sinus venosus and atrium well-developed in dorso-posterior position with respect to the ventricle. AA, Aortic arches; A, Atrium; IFT, Inflow tract; OFT, Outflow tract; SV, Sinus venosus; V, Ventricle. Magnification: $\times 250$ (d), $\times 180$ (c), $\times 300$ (a), $\times 400$ (b)



25 (Figures 1d–f, 2a–c). From GS 30, the atrium increased in size, doubling the ventricle size at GS 38 (Figure 2d–f). Melanophores were observed on the surface of the aortic arches, the outflow tract, the atrium, and the sinus venosus, but were absent on the surface of ventricle. Likewise, a progressive increase in the number of melanophores in the parietal pericardium was observed during the prometamorphic period.

Metamorphic larval period

During this period, important changes were observed in the topography and morphology of the heart and aortic arches. A displacement of the atrium and sinus venosus toward the anterior region was observed from GS 42 (Figure 2g). Likewise, between GS 43 and 46 (Figure 2h–k), the sinus venosus decreased in size and at the end of metamorphosis, it was located dorsally between the two atriums. At the end of metamorphosis, the configuration of the heart and aortic arches was similar to that of the adult

stage and the parietal pericardium was fully pigmented (Figure 2l).

3.1.2 | *Elachistocleis bicolor*

Embryonic period

Regionalization of the heart tube into the outflow tract, ventricle, and inflow tract was observed. Early (GS 19) and advanced stages (GS 20) of rightward looping were recognized (Figure 3a,b).

Premetamorphic larval period

The looping process continued from GS 21 up to the end of the metamorphic larval period, whereas the atrium showed a dorso-anterior position to the ventricle at GS 25 (Figure 3d). No melanophores were observed on the heart surface. A thin and translucent parietal pericardium was recognized at GS 24.

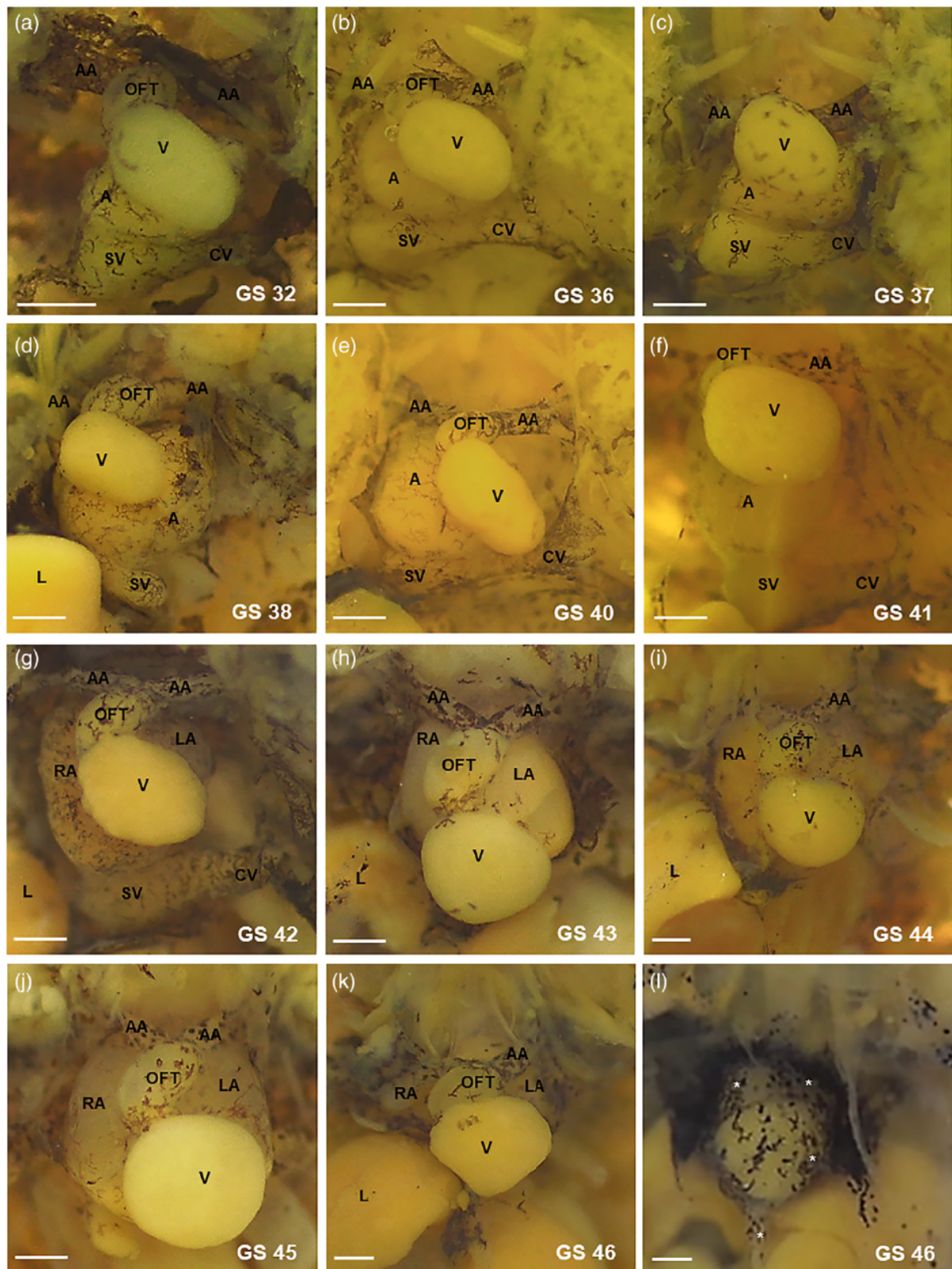


FIGURE 2 Heart morphology of *Physalaemus albonotatus* at prometamorphic (a–f) and metamorphic (g–k) larval periods. In (a–k) the parietal pericardium was removed to observe the heart structure. l) Detail of heart covered with the parietal pericardium, note the melanophores. AA, aortic arches; A, atrium; CV, Cardinal vein; L, Liver; LA, Left atrium; OFT, Outflow tract; RA, Right atrium; SV, Sinus venosus; V, Ventricle, *, Melanophores. Scale bar: 0.25 mm

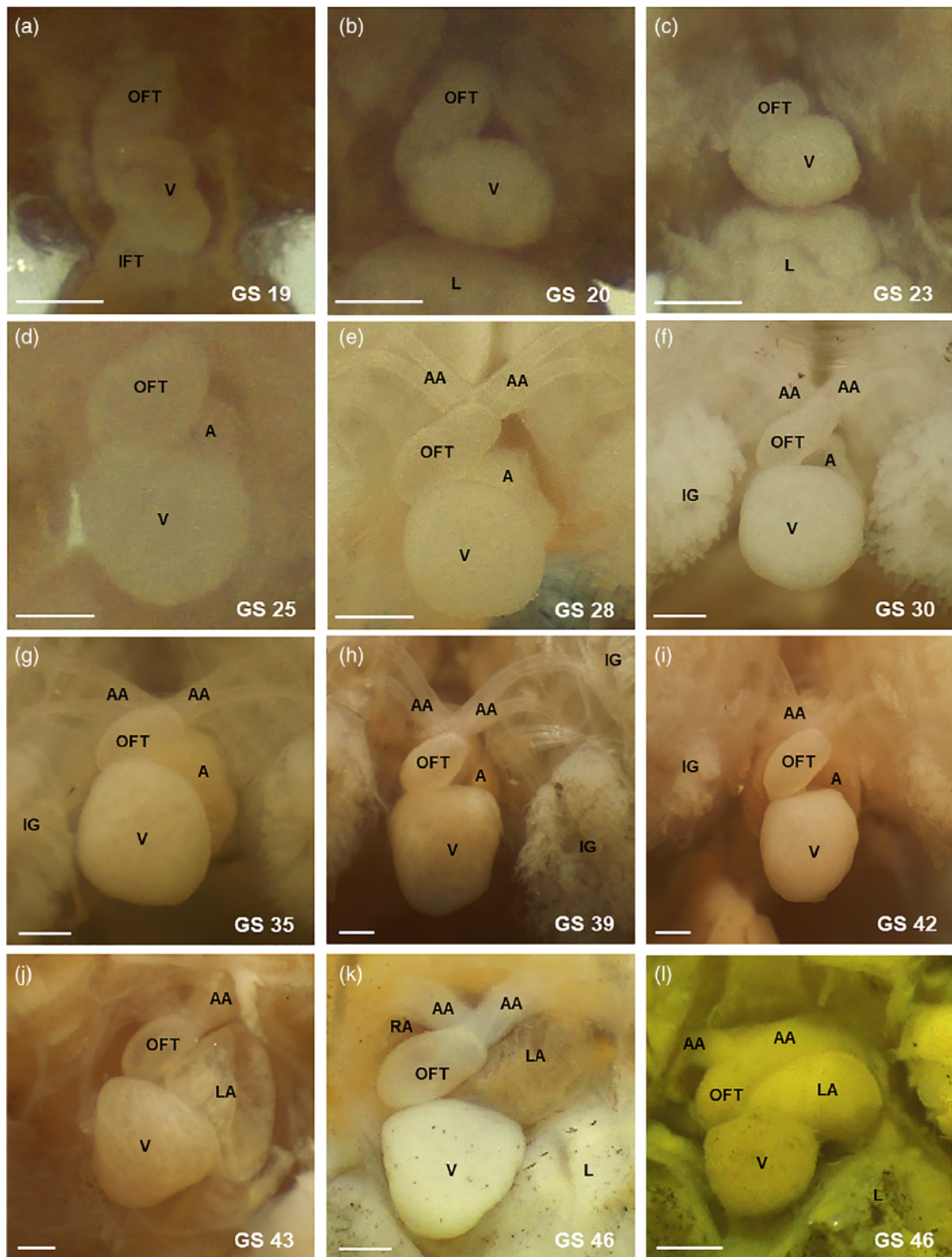


FIGURE 3 Heart morphology of *Elachistocleis bicolor* at the embryonic period (a, b) and premetamorphic (c, d), prometamorphic (e–i), and metamorphic (j–l) larval periods. In (a–k) the parietal pericardium was removed to observe the heart structure. (l) Detail of heart covered with the parietal pericardium. Note the absence of melanophores. AA, aortic arches; A, atrium; IFT, Inflow tract; IG, Internal gills; L, Liver; LA, Left atrium; OFT, Outflow tract; RA, Right atrium; SV, Sinus venosus; V, Ventricle. Scale bar: 0.25 mm

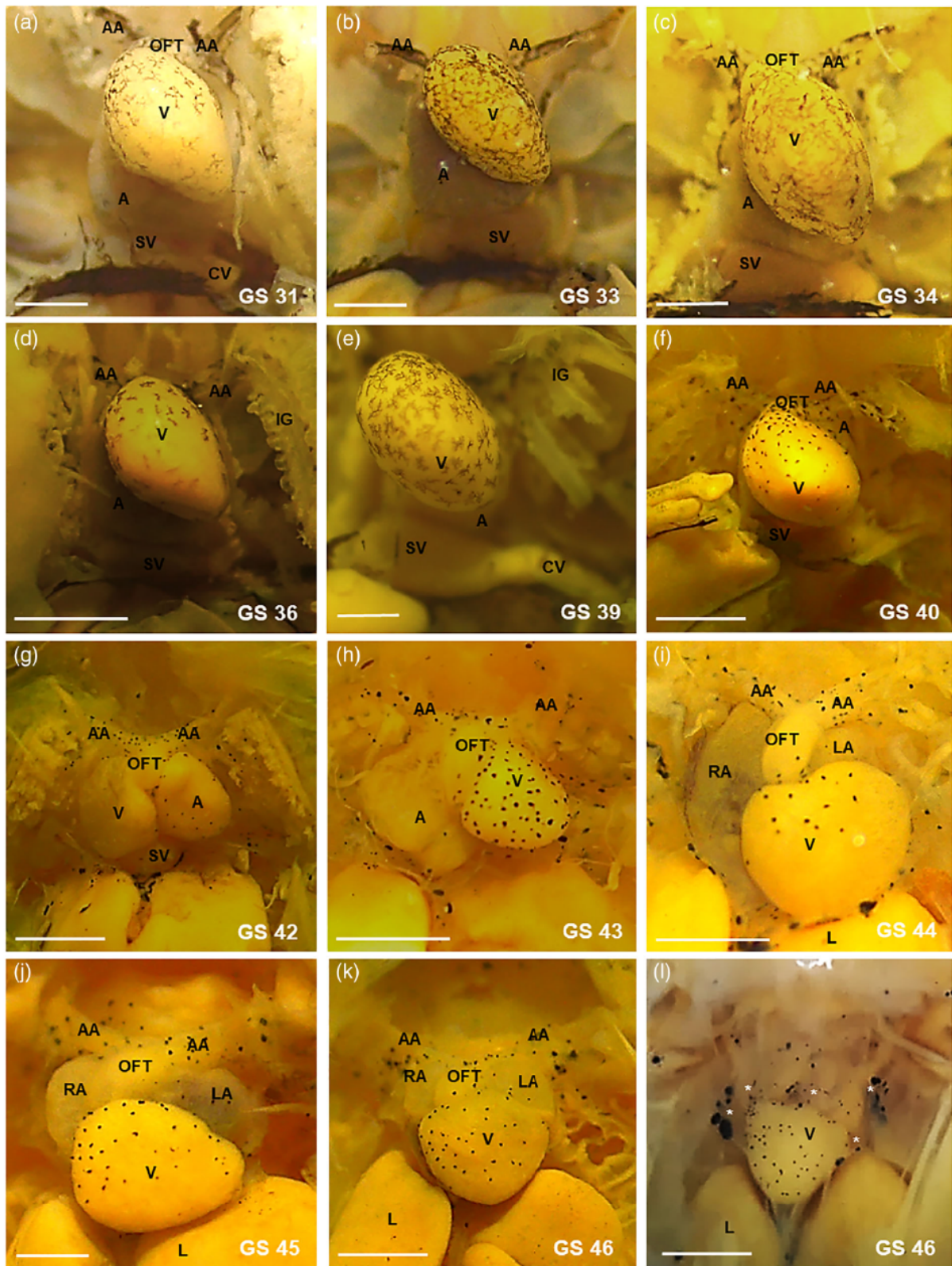
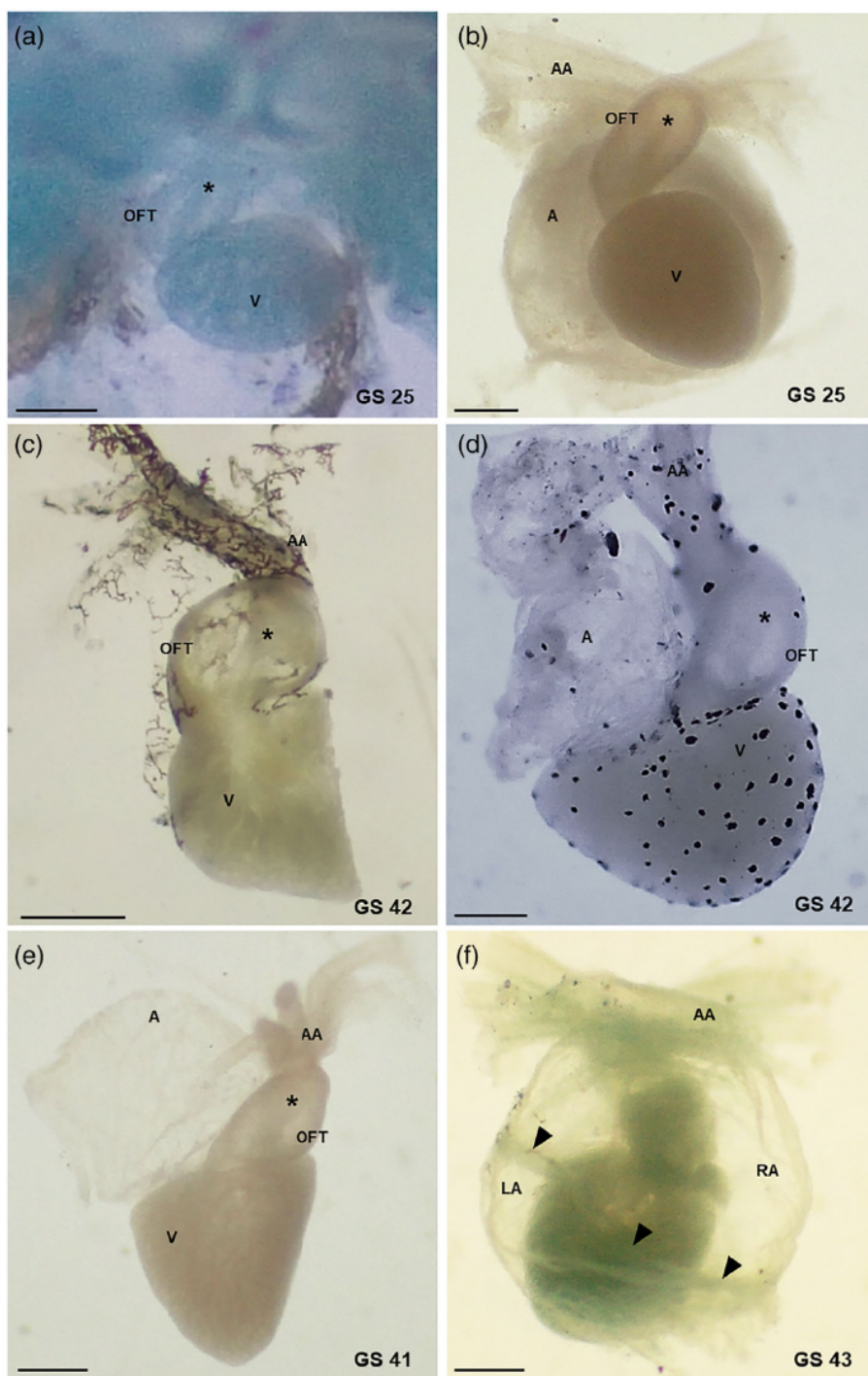


FIGURE 4 Heart morphology of *Scinax nasicus* at prometamorphic (a–f) and metamorphic (g–l) larval periods. In (a–k) the parietal pericardium was removed to observe the heart structure. (l) Detail of heart covered with the parietal pericardium. Note the melanophores. AA, aortic arches; A, atrium; CV, Cardinal vein; IG, Internal gills; L, Liver; LA, Left atrium; OFT, Outflow tract; RA, Right atrium; SV, Sinus venosus; V, Ventricle; *, Melanophores. Scale bar: a–c, e, f, k, l: 0.50 mm, d, g, h, i, j: 1 mm

FIGURE 5 Details of the spiral valve of *Physalaemus albonotatus* (a, c), *Scinax nasicus* (d), and *Elachistocleis bicolor* (b, e), and of the interatrial septum of *Elachistocleis bicolor*. (a, b) Ventral view of heart at GS 25. Note the thin spiral valve. (c) Sagittal section of heart at GS 42. Note the outflow tract with a well-developed spiral valve. (d) Right lateral view of heart at GS 42. Note the spiral valve inside the outflow tract. (e) Right lateral view of heart at GS 41 showing a single atrium. (f) Dorsal view of heart at GS 43. Note the interatrial septum (black arrowhead) separating the left and right atriums. A, Atrium; LA, Left atrium; OFT, Outflow tract; RA, Right atrium; SV, Sinus venosus; V, Ventricle; *, Spiral valve. Scale bar: a, 0.1 mm; b–f, 0.25 mm



Prometamorphic larval period

From GS 26 to 41, the heart morphology was similar to that in previous stages. The outflow tract was oblong and had an oblique position from left to right. The ventricle was prominent and oblong, rounded, or irregular in shape, and the endocardial trabeculae were observed. The atrium and sinus venosus had dorso-anterior position to the ventricle (Figure 3e–k). Melanophores were

absent on the heart surface as well as in the parietal pericardium (Figure 3l).

Metamorphic larval period

Between GS 42 and 46, no topographic changes were observed with respect to prometamorphic period (Figure 3i–k). However, an increase in atrium size was observed; thus, the atrium was observable on both sides

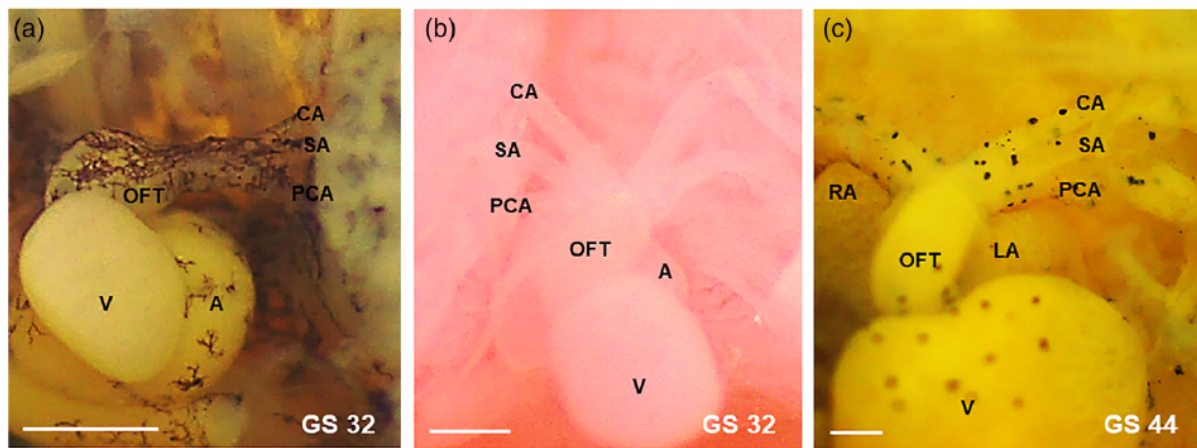


FIGURE 6 Aortic arches of *Physalaemus albonotatus* (a), *Elachistocleis bicolor* (b), and *Scinax nasicus* (c) during larval period. A, Atrium; CA, Carotid arch; LA, Left atrium; PCA, Pulmocutaneous arch; OFT, Outflow tract; RA, Right atrium; SA, Systemic arch; V, Ventricle. Scale bar: 0.25 mm

of the ventricle. Due to its dorsal position, the sinus venosus was not visible in ventral view. A few and small punctate-like melanophores, scattered on the surface of the ventricle, atrium, and sinus venosus were observed. No melanophores on the surface of outflow tract, aortic arches, or the parietal pericardium were observed (Figure 3l).

3.1.3 | *Scinax nasicus*

Prometamorphic larval period

Between GS 31 and 41, the ventricle was prominent and oblong and was in an oblique position. The sinus venosus and atrium showed a dorso-anterior position to the ventricle (Figure 4a-f). Abundant and dendritic or punctate-like melanophores were visible in the parietal pericardium and on the surface of the ventricle, outflow tract, and aortic arches. They were absent on the surface of sinus venosus and atrium.

Metamorphic larval period

The ventricle was prominent and irregular in shape. From GS 42 to GS 46, topographic changes of the sinus venosus and the atrium were observed (Figure 4g-k). These compartments were located in a dorso-anterior position to the ventricle at GS 43. Abundant melanophores were observed on the surface of the ventricle, outflow tract, and aortic arches, but they were scarce in the atrium. The parietal pericardium was fully pigmented (Figure 4l).

Spiral valve and atrial configuration

In *P. albonotatus* and *E. bicolor*, the spiral valve was observed as a thin membrane inside the outflow tract at

GS 25 (Figure 5a,b). In the three analyzed species, a well-developed spiral valve was observed at prometamorphic and metamorphic larval stages (Figure 5c-e).

In *P. albonotatus*, the atrium was a single chamber up to GS 43 and the left and right atriums were identified from GS 45. In *E. bicolor* the atrium remained as a single chamber up to GS 41 (Figure 5e), whereas the interatrial septum and the left and right atriums were evident from GS 43 (Figure 5f). This pattern was also observed in *S. nasicus*.

Aortic arches

The arrangement of the aortic arches during the embryonic period and prometamorphic and prometamorphic larval periods was similar in the three analyzed species (Figure 6). From the outflow tract, two short aortic arches extended on the right and left sides of the body. Each aortic arch was branched out into: carotid arch (III), systemic arch (IV) and pulmocutaneous arch (common stem of V and VI). These vessels correspond to the afferent arteries that supply blood to branchial arches: I, II, III, and IV ceratobranchial cartilages. From GS 45, the regression of the internal gills and changes in the arrangement of the aortic arches were observed. At the end of metamorphosis, the carotid, systemic and pulmocutaneous arteries were identified on each side of the body.

Critical periods of heart development

The main morphogenetic events occur during the embryonic and metamorphic periods (Figure 7). The formation of the heart tube, the rightward looping, the regionalization of the heart compartments, and the onset of heart-beat, take place at the embryonic period. The final

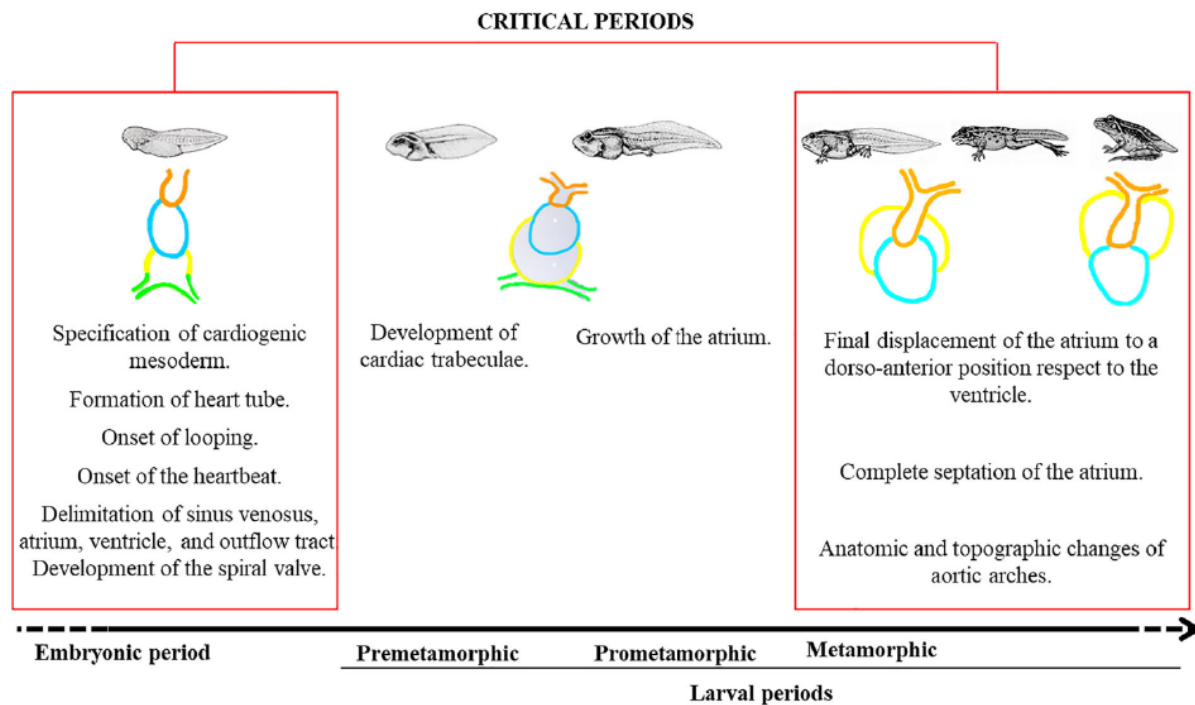


FIGURE 7 Critical periods of heart development based on the morphogenetic events observed in *Physalaemus albonotatus*

displacement of the atrium and its complete septation into the right and left atrium occur during metamorphosis. Consequently, these periods are critical for the heart development and function.

4 | DISCUSSION

Amphibian heart morphology shows significant variation among the orders and offers a source for unique adaptations to specific ways of life (Kraus & Metscher, 2021). In the present study, heart development during embryonic and larval development and metamorphosis of *P. albonotatus*, *E. bicolor*, and *S. nasicus* was characterized and compared. The general morphogenetic pattern was similar to that in other vertebrates and supports that heart development is conserved among vertebrates (Jensen et al., 2013).

During the embryonic period, the heart tube is formed and regionalized into four primordial compartments: outflow tract, ventricle, atrium, and sinus venosus. In addition, the looping process and the heartbeat start in this period. In *P. albonotatus* and *E. bicolor*, the looping takes place at about GS 18–23. In *P. albonotatus* this process stops during the premetamorphic larval period (GS 23), and the atrium remains dorso-posteriorly to the ventricle until the prometamorphic larval period. Since GS 38 the displacement of the atrium and sinus venosus continues. At the end of

metamorphosis, they acquire a dorso-anterior position with respect to the ventricle, similar to the topographic arrangement of the adult. This pattern was also observed in *S. nasicus* prometamorphic tadpoles. In contrast, in *E. bicolor* the displacement of the atrium and sinus venosus is continuous during the premetamorphic larval period and reaches its final topographic position at approximately GS 25. This pattern was previously described for *X. laevis* (Mohun et al., 2000).

Adults of anurans with well-developed lungs possess a complete interatrial septum and a spiral valve in the outflow tract that separate arterial and venous bloodstreams. The spiral valve guides the deoxygenated blood into the pulmocutaneous arch and the oxygenated blood into systemic and carotid arches during ventricular systole (Heinz-Taheny, 2009). In *X. laevis* the spiral valve develops early during the embryonic period, between Nieuwkoop and Faber stages 41–44 (Kolker et al., 2000; Lee & Saint-Jeannet, 2011; Mohun et al., 2000). In *P. albonotatus* and *E. bicolor*, a well-developed spiral valve was recognized at premetamorphic larval stages, presenting a similar development to *X. laevis*. In *S. nasicus*, it was not possible to analyze premetamorphic larval stages, but a conspicuous spiral valve was observed at prometamorphic larval stages. It is assumed that it follows the same morphogenetic pattern described for the other species.

Regarding to the atrial configuration, in *R. temporaria* (Viertel & Richter, 1999) and *X. laevis* (Jahr &

Männer, 2011; Mohun et al., 2000), the atrial septation ends during the premetamorphic larval period, approximately at GS 24. In *Rana pipiens* the first sign of interatrial septum was observed at Shumway stage 24 and was complete 1 month later (Jaffee, 1963). In *P. albonotatus*, *E. bicolor* and *S. nasicus*, as in the metamorphic axolotl, *Ambystoma mexicanum* (Olejnickova et al., 2021), the complete septation was evident during the metamorphic period. Moreover, heterochronic differences in the configuration of atriums were identified in these species. In *E. bicolor* and *S. nasicus*, the right and left atriums were evident early in metamorphosis (GS 43), whereas in *P. albonotatus* they were identified at the last metamorphic stages (GS 45 and 46). These changes in heart morphology involve physiological shifts of the circulatory and respiratory systems required for aquatic-terrestrial transition. Katano et al. (2019) state that the oxygen concentration affects the expression of genes involved in the heart septation playing an important role in cardiac morphogenesis. The knowledge of the ontogenetic changes during amphibian metamorphosis provides valuable insight into the evolution of the cardiovascular system (Olejnickova et al., 2021) and may help to interpret how the environmental factors regulate the heart structure and function. The differences in the timing of complete atrial septation, premetamorphic versus metamorphic periods, raise a question about the heart morphogenesis of larvae that needs to be analyzed in more depth.

The melanophores constitute an extracutaneous pigmentary system that shows a species-specific pattern (Zieri et al., 2007). Their presence, number, and morphology are highly variable between species (Franco-Belussi et al., 2011) and this variation depends on endogenous and environmental factors such as temperature, relative humidity, solar radiation, wind, rain, and photoperiod (Moresco & de Oliveira, 2009; Provete et al., 2012). In this study, interspecific differences in the pigmentation pattern of the heart were observed. In *P. albonotatus*, melanophores were present from prometamorphic larval period on the surface of the aortic arches, outflow tract, atrium, sinus venosus, and parietal pericardium, but the ventricle remained unpigmented up to the end of metamorphosis. In *S. nasicus* the melanophores were abundant in the parietal pericardium and on the surface of the ventricle, outflow tract, and aortic arches, but were absent in the atrium during the premetamorphic and metamorphic larval periods. However, in *E. bicolor* pigmentation was evident at the metamorphic larval period. Scarce melanophores were present mainly on the surface of the ventricle, but were absent in the parietal pericardium. Franco-Belussi et al. (2017) conclude that the pigmentation of the internal organs of anurans has a protective function and responds to climatic variables, depending

on the lineage and distribution of species. This conclusion could explain the variability observed in the three species analyzed in our study.

A teratogen agent produces malformations depending on the stage sensitivity, which can vary during development (Brent & Beckman, 1990). Exposure of embryos to teratogens during the early period of development may result in heart malformations (Sadler, 2017). Several studies in anurans have described heart defects, such as pericardial edema, cardioproptosis, cardiomegaly, and atrium reduction, because of exposure to a variety of toxic agents during the early stages of development (Calevro et al., 1998; Flach et al., 2022; Kim et al., 2013; Luo et al., 1993; Plowman et al., 1991). In addition, the cardiac physiology of anuran has been recognized as a sensitive endpoint in ecotoxicological studies involving sublethal exposure of an environmental stressor (Costa et al., 2008; Lajmanovich et al., 2019; Peltzer et al., 2019; Salla et al., 2016). The results of this study show that the main morphogenetic events and changes in heart morphology and topography occur during embryonic and metamorphic periods. Both periods are critical for the development of normal morphogenesis and the correct functioning of the anuran heart. These results are also useful to characterize the normal anuran heart morphology and to identify the possible abnormalities caused by exposure to environmental contaminants.

5 | CONCLUSION

The present study contributes evidence regarding the conserved morphogenetic pattern of heart development among anurans. In addition, heterochronic pathways were identified between *P. albonotatus* and *S. nasicus* compared to *E. bicolor*. Phylogenetic distances are likely to be responsible for the observed differences in heart development. Microhylidae larvae accumulate abundant apomorphic features, some of which are unique among anuran larvae (Haas, 2003). Heart morphogenesis may be another particular feature of this anuran family. Further studies of morphogenetic patterns in anuran species of different lineages and ecological habits are necessary to interpret these different developmental trajectories. Finally, our results could be useful to identify heart morphological and/or physiological abnormalities caused by exposure to environmental contaminants and to predict the potential risk for vertebrates.

ACKNOWLEDGMENTS

This work was supported by SGCyT-UNNE (20F002) and CAI+D (50620190100036LI), projects. We thank to Microscopia Electrónica de Barrido Service lab (SGCyT-

UNNE). Anonymous reviewers made valuable suggestions that greatly improved the early versions of this manuscript. We also thank J. Brasca for English editing and comments.

CONFLICT OF INTEREST

The authors declare no competing interests.

AUTHOR CONTRIBUTIONS

Sandoval María Teresa: Conceptualization (equal); formal analysis (equal); investigation (equal); methodology (equal); writing – original draft (equal); writing – review and editing (equal). **Gaona Romina:** Conceptualization (equal); formal analysis (equal); investigation (equal); methodology (equal); writing – original draft (equal). **Curi Lucila Marilén:** Writing – original draft (equal); writing – review and editing (equal). **Abreliano Fernanda:** Methodology (supporting). **Lajmanovich Rafael Carlos:** Supervision (equal); writing – review and editing (equal). **Peltzer Paola Mariela:** Supervision (equal); writing – review and editing (equal).

ETHICS STATEMENT

All procedures with the animals were approved by the Ethics Committee of the Facultad de Ciencias Exactas y Naturales y Agrimensura - UNNE (Res. 0756/18 CD).

DATA AVAILABILITY STATEMENT

The data that support the findings of this work are available from the corresponding author, upon reasonable request.

ORCID

María Teresa Sandoval  <https://orcid.org/0000-0003-1682-2255>

REFERENCES

- Bartman, T., & Hove, J. (2005). Mechanics and function in heart morphogenesis. *Developmental Dynamics: An Official Publication of the American Association of the Anatomists*, 233(2), 373–381.
- Brand, T. (2003). Heart development: Molecular insights into cardiac specification and early morphogenesis. *Developmental Biology*, 258(1), 1–19.
- Brent, R. L., & Beckman, D. A. (1990). Environmental teratogens. *Bulletin of the New York Academy of Medicine*, 66(2), 123–163.
- Calevro, F., Campani, S., Raghianti, M., Bucci, S., & Mancino, G. (1998). Tests of toxicity and teratogenicity in biphasic vertebrates treated with heavy metals (Cr³⁺, Al³⁺, Cd²⁺). *Chemosphere*, 37(14–15), 3011–3017.
- Casco, V. H., & Lajmanovich, R. C. (1999). *Atlas Histo-Embriológico de los principales estadios organogénicos de Physalaemus biligonigerus (Amphibia: Leptodactylidae)*. Museo Provincial de Ciencias Naturales Florentino Ameghino.
- Colas, J. F., Lawson, A., & Schoenwolf, G. C. (2000). Evidence that translation of smooth muscle alpha-Actin mRNA is delayed in the chick promyocardium until fusion of the bilateral heart-forming regions. *Developmental Dynamics*, 218(2), 316–330.
- Costa, M. J., Monteiro, D. A., Oliveira-Neto, A. L., Rantin, F. T., & Kalinin, A. L. (2008). Oxidative stress biomarkers and heart function in bullfrog tadpoles exposed to roundup original. *Ecotoxicology*, 17(3), 153–163.
- Cuzziol Boccioni, A. P., Peltzer, P. M., Martinuzzi, C. S., Attademo, A. M., León, E. J., & Lajmanovich, R. C. (2020). Morphological and histological abnormalities of the Neotropical toad, *Rhinella arenarum* (Anura: Bufonidae) larvae exposed to dexamethasone. *Journal of Environmental Science and Health, Part B*, 56(1), 41–53.
- Flach, H., Lenz, A., Pfeffer, S., Kühl, M., & Kühl, S. J. (2022). Impact of glyphosate-based herbicide on early embryonic development of the amphibian *Xenopus laevis*. *Aquatic Toxicology*, 244, 106081.
- Franco-Belussi, L., de Souza Santos, L. R., Zieri, R., & de Oliveira, C. (2011). Visceral pigmentation in four *Dendropsophus* species (Anura: Hylidae): Occurrence and comparison. *Zoologischer Anzeiger*, 250(2), 102–110.
- Franco-Belussi, L., Provete, D. B., & de Oliveira, C. (2017). Environmental correlates of internal coloration in frogs vary throughout space and lineages. *Ecology and Evolution*, 7(22), 9222–9233.
- Gosner, K. L. (1960). A simplified table for staging anuran embryos and larvae with notes on identification. *Herpetologica*, 16, 183–190.
- Haas, A. (2003). Phylogeny of frogs as inferred from primarily larval characters (Amphibia: Anura). *Cladistics*, 19, 23–89.
- Harvey, R. (2002). Patterning the vertebrate heart. *Nature Reviews Genetics*, 3, 544–556.
- Heinz-Taheny, K. M. (2009). Cardiovascular physiology and diseases of amphibians. *The Veterinary Clinics of North America. Exotic Animal Practice*, 12(1), 39–50.
- Hempel, A., & Kühl, M. (2016). A matter of the heart: The African clawed frog *Xenopus* as a model for studying vertebrate cardiogenesis and congenital heart defects. *Journal of Cardiovascular Development and Disease*, 3(2), 21.
- Incardona, J. P., & Scholz, N. L. (2017). Environmental pollution and the fish heart. *Fish Physiology*, 36(B), 373–433.
- Jaffee, O. C. (1963). Bloodstreams and the formation of the interatrial septum in the anuran heart. *The Anatomical Record*, 147(3), 355–357.
- Jahr, M., & Männer, J. (2011). Development of the venous pole of the heart in the frog *Xenopus laevis*: A morphological study with special focus on the development of the venoatrial connections. *Developmental Dynamics*, 240(6), 1518–1527.
- Jensen, B., Wang, T., Christoffels, V. M., & Moorman, A. F. (2013). Evolution and development of the building plan of the vertebrate heart. *Biochimica et Biophysica Acta (BBA)-molecular. Cell Research*, 1833(4), 783–794.
- Jones-Costa, M., Franco-Belussi, L., Vidal, F. A. P., Gongora, N. P., Castanho, L. M., dos Santos, C. C., Silva-Zacarin, C. E. M. F., Abdalla, F. C., Silveira Duarte, E. C., De Oliveira, C., de Oliveira, C. R., & Salla, R. F. (2018). Cardiac biomarkers as sensitive tools to evaluate the impact of xenobiotics on amphibians: The effects of anionic surfactant linear alkylbenzene

- sulfonate (LAS). *Ecotoxicology and Environmental Safety*, 151, 184–190.
- Katano, W., Moriyama, Y., Takeuchi, J. K., & Koshiba-Takeuchi, K. (2019). Cardiac septation in heart development and evolution. *Development, Growth & Differentiation*, 61(1), 114–123.
- Kim, M., Son, J., Park, M. S., Ji, Y., Chae, S., Jun, C., Bae, J. S., Kwon, T. K., Choo, Y. S., Yoon, H., Yoon, D., Ryoo, J., Kim, S. H., Park, M. J., & Lee, H. S. (2013). In vivo evaluation and comparison of developmental toxicity and teratogenicity of perfluoroalkyl compounds using *Xenopus* embryos. *Chemosphere*, 93(6), 1153–1160.
- Kolker, S. J., Tajchman, U., & Weeks, D. L. (2000). Confocal imaging of early heart development in *Xenopus laevis*. *Developmental Biology*, 218(1), 64–73.
- Kraus, N., & Metscher, B. (2021). Anuran heart metamorphosis: Anatomical support for pulmonary blood separation in the early aquatic phase. *The Anatomical Record*, 2021, 1–12.
- Lajmanovich, R. C., Peltzer, P. M., Martinuzzi, C. S., Attademo, A. M., Bassó, A., & Colussi, C. L. (2019). Insecticide pyriproxyfen (Dragón®) damage biotransformation, thyroid hormones, heart rate, and swimming performance of *Odontophrynus americanus* tadpoles. *Chemosphere*, 220, 714–722.
- Lavilla, E. O., & Rougés, M. (1992). Modos de reproducción de anuros argentinos. *Serie Divulgación. Asociación Herpetológica Argentina*, 5, 1–66.
- Leary S, Underwood W, Anthony R, Cartner S, Corey D, Grandin T, Greenacre C, Gwaltney-Brant S, McCrackin MA, Meyer R, Shearer DM, Yanong R. 2013. *AVMA guidelines for the euthanasia of animals 2013 edition*. Schaumburg: American Veterinary Medical Association.
- Lee, Y. H., & Saint-Jeannet, J. P. (2011). Cardiac neural crest is dispensable for outflow tract septation in *Xenopus*. *Development*, 138(10), 2025–2034.
- Lenkowski, J. R., Reed, J. M., Deininger, L., & McLaughlin, K. A. (2008). Perturbation of organogenesis by the herbicide atrazine in the amphibian *Xenopus laevis*. *Environmental Health Perspectives*, 116, 223–230.
- Linask, K. K., Han, M. D., Artman, M., & Ludwig, C. A. (2001). Sodium-calcium exchanger (NCX-1) and calcium modulation: NCX protein expression patterns and regulation of early heart development. *Developmental Biology*, 246, 407–417.
- Luo, S. Q., Plowman, M. C., Hopfer, S. M., & Sunderman, F. W. (1993). Embryotoxicity and teratogenicity of Cu²⁺ and Zn²⁺ for *Xenopus laevis*, assayed by the FETAX procedure. *Annals of Clinical and Laboratory Science*, 23(2), 111–120.
- Männer, J. (2009). The anatomy of cardiac looping: A step towards the understanding of the morphogenesis of several forms of congenital cardiac malformations. *Clinical Anatomy*, 22(1), 21–35.
- McIndoe, R., & Smith, D. G. (1984). Functional anatomy of the internal gills of the tadpole of *Litoria ewingii* (Anura, Hylidae). *Zoomorphology*, 104(5), 280–291.
- Miquerol, L., & Kelly, R. G. (2013). Organogenesis of the vertebrate heart. *Wiley Interdisciplinary Reviews: Developmental Biology*, 2(1), 17–29.
- Mohun, T. J., Leong, L. M., Weninger, W. J., & Sparrow, D. B. (2000). The morphology of heart development in *Xenopus laevis*. *Developmental Biology*, 218(1), 74–88.
- Moresco, R. M., & de Oliveira, C. (2009). A comparative study of the extracutaneous pigmentary system in three anuran amphibian species evaluated during the breeding season. *South American Journal of Herpetology*, 4(1), 1–8.
- Nemer, M. (2008). Genetic insights into normal and abnormal heart development. *Cardiovascular Pathology*, 17(1), 48–54.
- Olejnickova, V., Kolesova, H., Bartos, M., Sedmera, D., & Gregorovicova, M. (2021). The tale-tell heart: Evolutionary tetrapod shift from aquatic to terrestrial life-style reflected in heart changes in axolotl (*Ambystoma mexicanum*). *Developmental Dynamics*, 2021, 1–11.
- Olson, E. N., & Srivastava, D. (1996). Molecular pathways controlling heart development. *Science*, 272(5262), 671–676.
- Opitz, J. M., & Clark, E. B. (2000). Heart development: An introduction. *American Journal of Medical Genetics*, 97(4), 238–247.
- Orton, G. L. (1953). The systematics of vertebrate larvae. *Systematic Zoology*, 2, 63–75.
- Ozeki, H., Shirai, S., Ikeda, K., & Ogura, Y. (1999). Critical period for retinoic acid-induced developmental abnormalities of the vitreous in mouse fetuses. *Experimental Eye Research*, 68(2), 223–228.
- Paz, D. A. (1987). *Análisis descriptivo y experimental de los procesos de diferenciación de área cardíaca de Bufo arenarum* (Tesis Doctoral no Publicada). Universidad de Buenos Aires, Argentina.
- Peltzer, P. M., Cuzziol Boccioni, A. P., Attademo, M. A., Martinuzzi, C. S., Colussi, C. L., & Lajmanovich, R. C. (2022). Risk of chlorine dioxide as emerging contaminant during SARS-CoV-2 pandemic: Enzyme, cardiac, and behavior effects on amphibians tadpoles. *Toxicology and Environmental Health Sciences*, 14, 47–57.
- Peltzer, P. M., Lajmanovich, R. C., Martinuzzi, C., Attademo, A. M., Curi, L. M., & Sandoval, M. T. (2019). Biototoxicity of diclofenac on two larval amphibians: Assessment of development, growth, cardiac function and rhythm, behavior and antioxidant system. *Science of the Total Environment*, 683, 624–637.
- Pérez-Pomares, J. M., González-Rosa, J. M., & Muñoz-Chápuli, R. (2009). Building the vertebrate heart—an evolutionary approach to cardiac development. *International Journal of Developmental Biology*, 53, 1427–1443.
- Plowman, M. C., Peracha, H., Hopfer, S. M., & Sunderman, F. W., Jr. (1991). Teratogenicity of cobalt chloride in *Xenopus laevis*, assayed by the FETAX procedure. *Teratogenesis, Carcinogenesis, and Mutagenesis*, 11(2), 83–92.
- Praskova, E., Plhalova, L., Chromcova, L., Stepanova, S., Bedanova, I., Blahova, J., Hostovsky, M., Skoric, M., Maršálek, P., Voslarova, E., & Svobodova, Z. (2014). Effects of subchronic exposure of diclofenac on growth, histopathological changes, and oxidative stress in zebrafish (*Danio rerio*). *The Scientific World Journal*, 2014, 645737.
- Provete, D. B., Franco-Belussi, L., De Souza Santos, L. R., Zieri, R., Moresco, R. M. I. A., Martins, I. A., De Almeida, S. C., & de Oliveira, C. (2012). Phylogenetic signal and variation of visceral pigmentation in eight anuran families. *Zoologica Scripta*, 41(6), 547–556.
- Pyron, R. A., & Wiens, J. J. (2011). A large-scale phylogeny of Amphibia including over 2,800 species, and a revised classification of extant frogs, salamanders, and caecilians. *Molecular Phylogenetics and Evolution*, 62, 543–583.

- Sadler, T. W. (2017). Establishing the embryonic axes: Prime time for teratogenic insults. *Journal of Cardiovascular Development and Disease*, 4(3), 15.
- Salla, R. F., Gamero, F. U., Rissol, R. Z., Dal-Medico, S. E., Castanho, L. M., dos Santos, C. C., Silva-Zacarin, E. C. M., Kalinin, A. L., Abdalla, F. C., & Costa, M. J. (2016). Impact of an environmental relevant concentration of 17 α -ethinylestradiol on the cardiac function of bullfrog tadpoles. *Chemosphere*, 144, 1862–1868.
- Sater, A. K., & Jacobson, A. G. (1989). The specification of heart mesoderm occurs during gastrulation in *Xenopus laevis*. *Development*, 105(4), 821–830.
- Schneider, C. A., Rasband, W. S., & Eliceiri, K. W. (2012). NIH image to ImageJ: 25 years of image analysis. *Nature Methods*, 9(7), 671–675.
- Sekhotha, M., Monyeki, K., & Sibuyi, M. (2016). Exposure to agrochemicals and cardiovascular disease: A review. *International Journal of Environmental Research and Public Health*, 13(2), 229.
- Sissman, N. J. (1970). Developmental landmarks in cardiac morphogenesis: Comparative chronology. *The American Journal of Cardiology*, 25, 141–148.
- Sorrivas de Lozano, V. S., & Morales, J. (1986). *Introducción a la microscopía electrónica*. CRIBABB.
- Tyser, R. C., & Srinivas, S. (2020). The first heartbeat-origin of cardiac contractile activity. *Cold Spring Harbor Perspectives in Biology*, 12, a037135.
- Vaira, M., Akmentins, M., Attademo, M., Baldo, D., Barrasso, D. A., Barrionuevo, S., Basso, N. G., Blotto Acuña, B. L., Cairo, S., Cajade, R., Céspedes, J. A., Chilote, P., Duré Pitteri, M. I., Falcione, A. C., Ferraro, D. P., Gutierrez, F. R., MdelR, L., Junges, C. M., Lajmanovich, R. C., ... Zaracho, V. H. (2012). Categorización del estado de conservación de los anfibios de la República Argentina. *Cuadernos de Herpetología*, 26, 131–159.
- Viertel, B., & Richter, S. (1999). Anatomy: Viscera and endocrines. In R. W. Mc Diarmid & R. Altig (Eds.), *Tadpoles: The biology of anuran larvae* (pp. 92–148). University of Chicago Press.
- Warkman, A. S., & Krieg, P. A. (2007). *Xenopus* as a model system for vertebrate heart development. *Seminars in Cell & Developmental Biology*, 18, 46–53.
- Watson, F. L., Schmidt, H., Turman, Z. K., Hole, N., García, H., Gregg, J., Tilghman, J., & Fradinger, E. A. (2014). Organophosphate pesticides induce morphological abnormalities and decrease locomotor activity and heart rate in *Danio rerio* and *Xenopus laevis*. *Environmental Toxicology and Chemistry*, 33(6), 1337–1345.
- Wittig, J. G., & Münsterberg, A. (2016). The early stages of heart development: Insights from chicken embryos. *Journal of Cardiovascular Development and Disease*, 3, 12.
- Wittig, J. G., & Münsterberg, A. (2020). The chicken as a model organism to study heart development. *Cold Spring Harbor Perspectives in Biology*, 12, a037218.
- Xavier-Neto, J., Davidson, B., Simoes-Costa, M. S., Castro, R. A., Castillo, H. A., Sampaio, A. C., & Azambuja, A. P. (2010). Evolutionary origins of hearts. In N. Rosenthal & R. P. Harvey (Eds.), *Heart development and regeneration* (pp. 3–45). Academic Press.
- Yunqing, S., Svetlana, K., Chenleng, C., & Sylvia, E. (2000). BMP signaling is required for heart formation in vertebrates. *Developmental Biology*, 224, 226–237.
- Zaracho, V. H., Céspedes, J. A., Álvarez, B. B., & Lavilla, E. O. (2011). *Anfibios de Corrientes. Guía de campo para la identificación de los Anfibios de la provincia de Corrientes Tucumán*. Fundación Miguel Lillo.
- Zieri, R., Taboga, S. R., & de Oliveira, C. (2007). Melanocytes in the testes of *Eupemphix nattereri* (Anura, Leiuperidae): Histological, stereological, and ultrastructural aspects. *The Anatomical Record: Advances in Integrative Anatomy and Evolutionary Biology*, 290(7), 795–800.

How to cite this article: Sandoval, M. T., Gaona, R., Curi, L. M., Abreliano, F., Lajmanovich, R. C., & Peltzer, P. M. (2022). Anuran heart development and critical developmental periods: A comparative analysis of three neotropical anuran species. *The Anatomical Record*, 1–15. <https://doi.org/10.1002/ar.24933>

